

Macroscopic evidence for quantum criticality and field-induced quantum fluctuations in cuprate superconductors

A. D. Beyer,¹ V. S. Zapf,² H. Yang,¹ F. Fabris,² M. S. Park,³ K. H. Kim,³ S.-I. Lee,³ and N.-C. Yeh¹

¹*Department of Physics, California Institute of Technology, Pasadena, CA*

²*National High Magnetic Field Laboratory, Los Alamos, NM*

³*Department of Physics, Pohang University of Science and Technology, Pohang, Korea*

(Dated: October 6, 2007)

We present *macroscopic* experimental evidence for field-induced *microscopic* quantum fluctuations in different hole- and electron-type cuprate superconductors with varying doping levels and numbers of CuO₂ layers per unit cell. The significant suppression of the zero-temperature in-plane magnetic irreversibility field relative to the paramagnetic field in all cuprate superconductors suggests strong quantum fluctuations due to the proximity of the cuprates to quantum criticality.

PACS numbers: 74.25.Dw, 74.72.-h, 74.25.Op, 74.40.+k

High-temperature superconducting cuprates are extreme type-II superconductors that exhibit strong thermal, disorder and quantum fluctuations in their vortex states.¹⁻⁹ While much research has focused on the *macroscopic* vortex dynamics of cuprate superconductors with phenomenological descriptions,^{1-5,7} little effort has been made to address the *microscopic* physical origin of their extreme type-II nature.⁹ Given that competing orders (CO) can exist in the ground state of these doped Mott insulators besides superconductivity (SC),⁹⁻¹⁵ the occurrence of quantum criticality may be expected.^{11,13,16} The proximity to quantum criticality and the existence of CO can significantly affect the low-energy excitations of the cuprates due to strong quantum fluctuations^{8,9} and the redistribution of quasiparticle spectral weight among SC and CO.^{9,17,18} Indeed, empirically the low-energy excitations of cuprate superconductors appear to be unconventional, exhibiting intriguing properties unaccounted for by conventional Bogoliubov quasiparticles.^{9,17-19} Moreover, external variables such as temperature (T) and applied magnetic field (H) can vary the interplay of SC and CO, such as inducing or enhancing the CO^{20,21} at the price of more rapid suppression of SC, thereby leading to weakened superconducting stiffness and strong thermal and field-induced fluctuations.¹⁻³ On the other hand, the quasi two-dimensional nature of the cuprates can also lead to quantum criticality in the limit of decoupling of CuO₂ planes. In this work we demonstrate experimental evidence from *macroscopic* magnetization measurements for field-induced quantum fluctuations among a wide variety of cuprate superconductors with different *microscopic* variables such as the doping level (δ) of holes or electrons, and the number of CuO₂ layers per unit cell (n).²² We suggest that the manifestation of strong field-induced quantum fluctuations is consistent with a scenario that all cuprates are in close proximity to a quantum critical point (QCP).⁶

To investigate the effect of quantum fluctuations on the vortex dynamics of cuprate superconductors, our strategy involves studying the vortex phase diagram at $T \rightarrow 0$ to minimize the effect of thermal fluctuations, and apply-

ing magnetic field *parallel* to the CuO₂ planes ($H \parallel ab$) to minimize the effect of random point disorder. The rationale for having $H \parallel ab$ is that the intrinsic pinning effect of layered CuO₂ planes generally dominates over the pinning effects of random point disorder, so that the commonly observed glassy vortex phases associated with point disorder for $H \parallel c$ (e.g. vortex glass and Bragg glass)^{1,5,7} can be prevented. In the *absence* of quantum fluctuations, random point disorder can cooperate with the intrinsic pinning effect to stabilize the low-temperature vortex smectic and vortex solid phases,⁴ so that the vortex phase diagram for $H \parallel ab$ would resemble that of the vortex-glass and vortex-liquid phases observed for $H \parallel c$ with a glass transition $H_G(T = 0)$ approaching $H_{c2}(T = 0)$. On the other hand, when *field-induced quantum fluctuations* are dominant, the vortex phase diagram for $H \parallel ab$ will deviate substantially from predictions solely based on thermal fluctuations and intrinsic pinning, and we expect strong suppression of the magnetic irreversibility field H_{irr}^{ab} relative to the upper critical field H_{c2}^{ab} at $T \rightarrow 0$, because the induced persistent current circulating along both the c -axis and the ab -plane can no longer be sustained if field-induced quantum fluctuations become too strong to maintain the c -axis superconducting phase coherence.

In this communication we present experimental results that are consistent with the notion that all cuprate superconductors exhibit significant field-induced quantum fluctuations as manifested by a characteristic field $H_{irr}^{ab}(T \rightarrow 0) \equiv H^* \ll H_{c2}^{ab}(T \rightarrow 0)$. Moreover, we find that we can express the degree of quantum fluctuations for each cuprate in terms of a reduced field $h^* \equiv H^*/H_{c2}^{ab}(0)$, with $h^* \rightarrow 0$ indicating strong quantum fluctuations and $h^* \rightarrow 1$ referring to the mean-field limit. Most important, the h^* values of all cuprates appear to follow a trend on a $h^*(\alpha)$ -vs.- α plot, where α is a material parameter for a given cuprate that reflects its doping level, electronic anisotropy, and charge imbalance if the number of CuO₂ layers per unit cell n satisfies $n \geq 3$.^{23,24} In the event that $H_{c2}^{ab}(0)$ exceeds the paramagnetic field $H_p \equiv \Delta_{SC}(0)/(\sqrt{2}\mu_B)$ for highly anisotropic

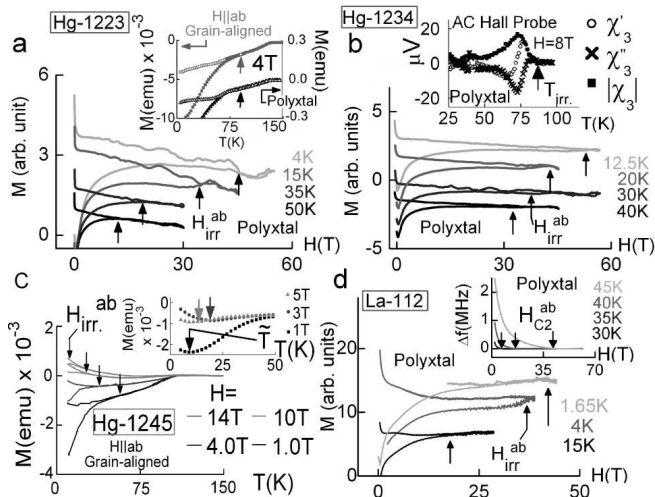


FIG. 1: Representative measurements of the in-plane irreversibility fields $H_{irr}^{ab}(T)$ in cuprate superconductors: (a) Hg-1223 (polycrystalline and grain-aligned), (b) Hg-1234 (polycrystalline), (c) Hg-1245 (grain-aligned), and (d) La-112 (polycrystalline and grain-aligned). Insets: (a) Consistent $T_{irr}^{ab}(H)$ obtained from maximum irreversibility of a polycrystalline sample and from irreversibility of a grain-aligned sample with $H \parallel ab$; (b) representative χ_3 data taken using AC Hall probe techniques; (c) details of the M -vs- T curves, showing an anomalous upturn at $T < \tilde{T}$; (d) exemplifying determination of H_{c2}^{ab} in La-112 using TDO to measure Δf .⁸

cuprates, where $\Delta_{SC}(0)$ denotes the superconducting gap at $T = 0$, h^* is defined by (H^*/H_p) because H_p becomes the maximum critical field for superconductivity.

To find h^* , we need to determine both the upper critical field $H_{c2}^{ab}(T)$ and the irreversibility field $H_{irr}^{ab}(T)$ to as low temperature as possible. Empirically, $H_{c2}^{ab}(T)$ can be derived from measuring the magnetic penetration depth in pulsed fields, with $H_{c2}^{ab}(0)$ extrapolated from $H_{c2}^{ab}(T)$ values obtained at finite temperatures. The experiments involve measuring the frequency shift Δf of a tunnel diode oscillator (TDO) resonant tank circuit with the sample contained in one of the component inductors. Details of the measurement techniques have been given in Ref. 8. In general we find that the condition $H_{c2}^{ab}(0) > H_p$ is satisfied among all samples investigated so that we define $h^* \equiv (H^*/H_p)$ hereafter. On the other hand, determination of $H_{c2}^{ab}(0)$ and $H_{c2}^c(0)$ is still useful because it provides the electronic anisotropy $\gamma \equiv (\xi_{ab}/\xi_c) = [H_{c2}^{ab}(0)/H_{c2}^c(0)]$, where $\xi_{ab}(\xi_c)$ refers to the in-plane (c -axis) superconducting coherence length.

To determine $H_{irr}^{ab}(T)$, we employed different experimental techniques, including DC measurements of the magnetization $M(T, H)$ with the use of a SQUID magnetometer or a homemade Hall probe magnetometer for lower fields (up to 9 Tesla), a DC magnetometer (up to 14 Tesla) at the National High Magnetic Field Laboratory (NHMFL) in Los Alamos (LANL-PPMS), a cantilever magnetometer at the NHMFL in Tallahassee for higher fields (up to 33 Tesla DC fields in a ³He refrigerator),²⁵

and a compensated coil for magnetization measurements in the pulsed-field (PF) facilities at LANL for even higher fields (up to 65 Tesla pulsed fields in a ³He refrigerator).⁸ In addition, AC measurements of the third harmonic magnetic susceptibility (χ_3) as a function of temperature in a constant field are employed to determine the onset of non-linearity in the low-excitation limit.²⁶ Examples of the measurements of $H_{irr}^{ab}(T)$ for HgBa₂Ca₂Cu₃O_x (Hg-1223, $T_c = 133$ K), HgBa₂Ca₃Cu₄O_x (Hg-1234, $T_c = 125$ K), HgBa₂Ca₄Cu₅O_x (Hg-1245, $T_c = 108$ K) and Sr_{0.9}La_{0.1}CuO₂ (La-112, $T_c = 43$ K), are shown in Fig. 1 (a) - (d), and the consistency among $H_{irr}^{ab}(T)$ deduced from different techniques have been verified, as summarized in the H -vs- T phase diagrams ($H \parallel ab$) in Fig. 2(a) - (d). The Hg-based cuprates are in either polycrystalline or grain-aligned forms, and the quality of these samples is confirmed with x-ray diffraction and magnetization measurements to ensure single phase and nearly 100% volume superconductivity.^{27,28} We have also verified that $H_{irr}^{ab}(T)$ obtained from the polycrystalline samples are consistent with those derived from the grain-aligned samples with $H \parallel ab$, because the measured irreversibility in a polycrystalline sample is manifested by its maximum irreversibility H_{irr}^{ab} among grains of varying orientation relative to the applied field. Examples of this consistency have been shown in Ref. 8 and also in the main panel and the inset of Fig. 1(a).

In addition to the four different cuprates considered in this work, we compare measurements of $H_{irr}^{ab}(T)$ on other cuprate superconducting single crystals, including underdoped YBa₂Cu₃O_{7- δ} (Y-123, $T_c = 87$ K),²⁹ optimally doped Nd_{1.85}Ce_{0.15}CuO₄ (NCCO, $T_c = 23$ K)³⁰ and overdoped Bi₂Sr₂CaCu₂O_x (Bi-2212, $T_c = 60$ K).³¹ The irreversibility fields for these cuprates normalized to their corresponding paramagnetic fields H_p are summarized in Fig. 3(a) as a function of the reduced temperature (T/T_c), clearly demonstrating strong suppression of H^* relative to H_p and $H_{c2}^{ab}(0)$ in all cuprates and implying significant field-induced quantum fluctuations.

The physical significance of h^* may be better understood by considering how the magnetic irreversibility for $H \parallel ab$ occurs. For sufficiently low T and small H , a supercurrent circulating both along and perpendicular to the CuO₂ planes with a coherent superconducting phase can be induced and sustained, leading to magnetic irreversibility. On the other hand, strong thermal or quantum fluctuations due to large anisotropy and competing orders in the cuprates can reduce the phase coherence of supercurrents, particularly the coherence perpendicular to the CuO₂ planes, thereby diminishing the magnetic irreversibility. Thus, we expect that the degree of the in-plane magnetic irreversibility is dependent on the nominal doping level δ , the electronic anisotropy γ , the number of CuO₂ layers per unit cell n , and the ratio of charge imbalance (δ_o/δ_i) ^{23,24} between the doping level of the outer layers (δ_o) and that of the inner layer(s) (δ_i) in multi-layer cuprates with $n \geq 3$. In other words, h^* for each cuprate superconductor may be expressed in terms

TABLE I: Quantum criticality parameters among different cuprates. All fields in tesla. σ denotes a parameter's uncertainty.

	δ	δ_o	δ_i	γ	σ_γ	$\alpha(10^{-2})$	$\sigma_\alpha(10^{-3})$	H^*	σ_{H^*}	$H_{c2}^{ab}[H_P]$	σ_{H_P}	h^*	σ_{h^*}
Hg-1245	0.15	1.30	0.80	55^{32}	25	0.06	0.3	23.0	5.0	-[278]	40	0.08	0.02
Hg-1223	0.15	1.04	0.92	52^{33}	18	0.26	0.9	48.5	6.5	-[347]	50	0.14	0.02
Hg-1234	0.15	1.20	0.80	52^{33}	10	0.13	0.2	75.0	10.0	-[320]	46	0.23	0.02
La-112	0.10	1.00	1.00	13^8	4.0	0.77	2.4	46.0	4.0	160[110]	10	0.42	0.04
Bi-2212	0.225	1.00	1.00	11^{31}	8.0	2.05	15	65.0	10	100[155]	22	0.42	0.06
NCCO	0.15	1.00	1.00	13^{30}	5.0	1.15	4.4	40.0	5.0	77[59]	8.0	0.68	0.12
Y-123	0.13	1.00	1.00	7.0^{33}	2.0	1.86	5.3	210	50	600[239]	25	0.88	0.23

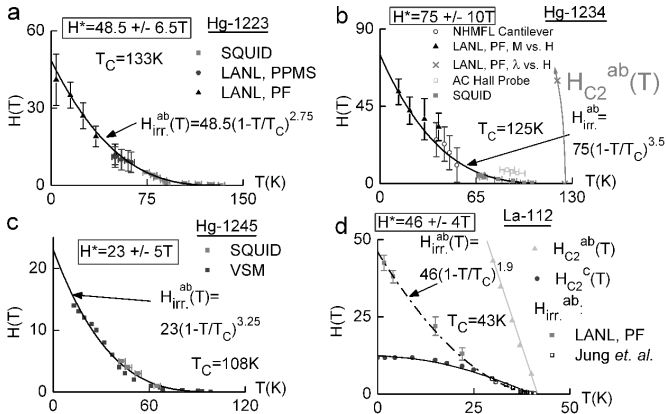


FIG. 2: Determination of H^* using various magnetic measurements of $H_{irr}^{ab}(T)$: (a) Hg-1223, (b) Hg-1234, (c) Hg-1245, and (d) La-112. In (b) and (d) dashed lines indicate $H_{c2}^{ab}(T)$ from TDO measurements. In (d) we also illustrate H_{c2}^c for comparison. We note reasonable consistency among different experimental techniques, indicating strong suppression of $H^* \equiv H_{irr}^{ab}(0)$ relative to $H_{c2}^{ab}(0)$ (or H_p) in all cuprates.

of a material parameter α that depends on δ , γ , n and (δ_o/δ_i) , and the simplest assumption for a linearized dependence of α on these variables gives:

$$\alpha \equiv \gamma^{-1} \delta (\delta_o/\delta_i)^{-(n-2)}, \quad (n \geq 3); \quad (1)$$

$$\alpha \equiv \gamma^{-1} \delta, \quad (n \leq 2). \quad (2)$$

If the suppression of the in-plane magnetic irreversibility is associated with field-induced quantum fluctuations and the proximity to a quantum critical point α_c ,¹¹ $h^*(\alpha)$ should be a function of $|\alpha - \alpha_c|$. Indeed, we find that using the empirically determined values for different cuprates tabulated in Table 1 and the definition of α given above, the h^* -vs.- α data for a wide variety of cuprates appear to follow a trend, as shown in Fig. 3(b). For comparison, we include in Fig. 3(b) theoretical curves predicted for field-induced static spin density waves (SDW) in cuprate superconductors in the limit of $H_{c1}(0) \ll H \ll H_{c2}(0)$, where h^* (above which static SDW coexists with SC) satisfies the relation:¹¹

$$h^*(\alpha) \propto |\alpha - \alpha_c| / [\ln |\alpha - \alpha_c|]. \quad (3)$$

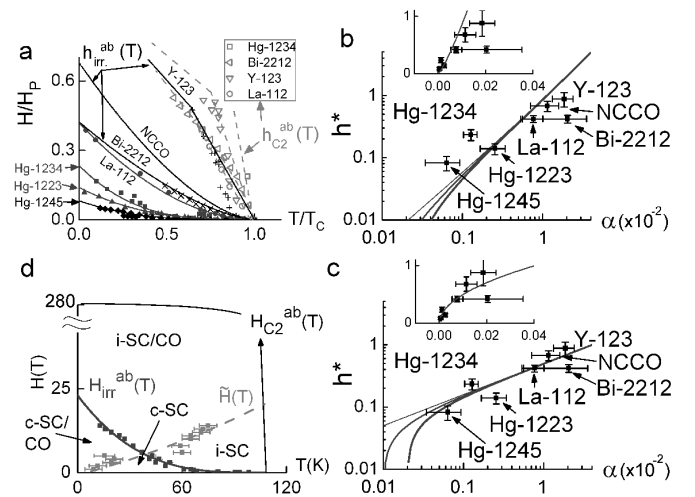


FIG. 3: (a) Reduced in-plane fields (H_{irr}^{ab}/H_p) and (H_{c2}^{ab}/H_p) vs. (T/T_c) for various cuprates. In the $T \rightarrow 0$ limit where $H_{irr}^{ab} \rightarrow H^*$, the reduced fields $h^* \equiv (H^*/H_p) < 1$ for all cuprates are listed in Table I for Y-123, NCCO, Bi-2212, La-112, Hg-1234, Hg-1223, and Hg-1245 (in descending order). (b) h^* vs. α in logarithmic plot for different cuprates, with decreasing α representing increasing quantum fluctuations. The lines given by $-400|\alpha - \alpha_c| / \ln |\alpha - \alpha_c|$ represent the field-induced SDW scenario¹¹ in Eq. (3) with different $\alpha_c = 0, 10^{-4}$ and 2×10^{-4} from left to right. Inset: The linear plot of the main panel. (c) The same data as in (b) are compared with the power-law dependence (solid lines) given by $5(\alpha - \alpha_c)^{1/2}$, using different $\alpha_c = 0, 10^{-4}$ and 2×10^{-4} from left to right. Inset: The linear plot of the main panel. (d) The H -vs.- T diagram of Hg-1245. (See text for details).

Here α_c is a non-universal critical point,¹¹ $h^*(\alpha) \rightarrow 0$ for $\alpha \rightarrow \alpha_c$, and we have shown theoretical curves associated with three different α_c values for comparison with data. On the other hand, a simple scaling argument would assert a power-law dependence:

$$h^*(\alpha) \propto |\alpha - \alpha_c|^a. \quad (a > 0) \quad (4)$$

Using $a \sim 0.5$ in Eq. (4), we compare the power-law dependence with experimental data in Fig. 3(c). This dependence appears to agree better with experimental data than the SDW/SC formalism in Eq. (3).

Although our available data cannot accurately determine α_c , we further examine Hg-1245 (which has the smallest h^*) for additional clues associated with the nature of the QCP. We find that the magnetization M of Hg-1245 always exhibits an anomalous increase for $T < T(H)$ (see the inset of Fig. 1(c)), indicating a field-induced reentry of magnetic ordering below $\tilde{T}(H)$. This magnetism reentry line $\tilde{H}(T)$ is shown together with $H_{irr}^{ab}(T)$ in Fig. 3(d). We suggest that the regime below both H_{irr}^{ab} and \tilde{H} corresponds to a coherent SC state (c -SC), and that bounded by H_{irr}^{ab} and \tilde{H} is associated with a coherent phase of coexisting SC and magnetic CO (c -SC/CO), whereas that above H_{irr}^{ab} is an incoherent SC phase (i -SC and i -SC/CO) with strong fluctuations.

Our conjecture of a field-induced magnetic CO in Hg-1245 contributing to quantum fluctuations may be further corroborated by considering the h^* -vs.- α dependence in the multi-layered cuprates Hg-1223, Hg-1234 and Hg-1245. While these cuprate superconductors have the highest T_c and H_{c2} values, as shown in Table I, they also exhibit the smallest h^* and α values, suggesting maximum quantum fluctuations. These strong quantum fluctuations can be attributed to both their extreme two dimensionality (i.e., large γ)^{27,34} and significant charge imbalance that leads to strong CO in the inner layers.^{23,24} Indeed muon spin resonance (μ SR) experiments³⁵ have revealed increasing antiferromagnetic ordering in the inner layers of the multi-layer cuprates with $n \geq 3$. Given that the γ values of all Hg-based multi-layer cuprates

are comparable (Table I), the finding of larger quantum fluctuations (i.e. smaller h^*) in Hg-1245 is suggestive of increasing quantum fluctuations with stronger competing order. However, further investigation of the h^* and γ values of other multi-layer cuprates will be necessary to confirm whether competing orders in addition to large anisotropy contribute to quantum fluctuations.

In summary, our investigation of the *in-plane* magnetic irreversibility in a wide variety of cuprate superconductors reveals strong field-induced quantum fluctuations. The *macroscopic* irreversibility field exhibits dependences on such *microscopic* material parameters as the doping level, the charge imbalance in multi-layered cuprates, and the electronic anisotropy. Our finding is consistent with the notion that cuprate superconductors are in close proximity to quantum criticality.

Acknowledgments

Research at Caltech was supported by NSF Grant DMR-0405088 and through the NHMFL. The SQUID data were taken at the Beckman Institute at Caltech. Work at Pohang University was supported by the Ministry of Science and Technology of Korea. The authors gratefully acknowledge Dr. Kazuyasu Tokiwa and Dr. Tsuneo Watanabe at the Tokyo University of Science for providing the HgBa₂Ca₄Cu₅O_x (Hg-1245) samples.

-
- ¹ D. S. Fisher, M. P. A. Fisher, and D. Huse, Phys. Rev. B **43**, 130 (1991).
 - ² G. Blatter, M. Feigel'man, V. Geshkenbein, A. Larkin, and V. Vinokur, Rev. Mod. Phys. **66**, 1125 (1994).
 - ³ N.-C. Yeh, W. Jiang, D. S. Reed, U. Kriplani, F. Holtzberg, C. C. Tsuei, and C. C. Chi, Physica A **200**, 374 (1993).
 - ⁴ L. Balents and D. R. Nelson, Phys. Rev. Lett. **73**, 2618 (1994).
 - ⁵ T. Giamarchi and P. L. Doussal, Phys. Rev. B **52**, 1242 (1995).
 - ⁶ G. Kotliar and C. M. Varma, Phys. Rev. Lett. **77**, 2296 (1996).
 - ⁷ J. Kierfeld and V. M. Vinokur, Phys. Rev. B **69**, 024501 (2004).
 - ⁸ V. S. Zapf, N.-C. Yeh, A. D. Beyer, C. R. Hughes, C. H. Mielke, N. Harrison, M. S. Park, K. H. Kim, and S.-I. Lee, Phys. Rev. B **71**, 134526 (2005).
 - ⁹ N.-C. Yeh, C.-T. Chen, V. S. Zapf, A. D. Beyer, and C. R. Hughes, Int. J. Mod. Phys. B **19**, 285 (2005).
 - ¹⁰ S.-C. Zhang, Science **275**, 1089 (1997).
 - ¹¹ E. Demler, S. Sachdev, and Y. Zhang, Phys. Rev. Lett. **87**, 067202 (2001).
 - ¹² S. Chakravarty, R. B. Lauhlin, D. K. Morr, and C. Nayak, Phys. Rev. B **63**, 094503 (2001).
 - ¹³ S. Sachdev, Rev. Mod. Phys. **75**, 913 (2003).
 - ¹⁴ S. Kivelson, I. Bindloss, E. Fradkin, V. Oganesyan, J. Tranquada, A. Kapitulnik, and C. Howald, Rev. Mod. Phys. **75**, 1201 (2003).
 - ¹⁵ P. A. Lee, N. Nagaosa, and X.-G. Wen, Rev. Mod. Phys. **78**, 17 (2006).
 - ¹⁶ F. Onufrieva and P. Pfeuty, Phys. Rev. Lett. **92**, 247003 (2004).
 - ¹⁷ C.-T. Chen, A. D. Beyer, and N.-C. Yeh, Solid State Communications **143**, 447 (2007).
 - ¹⁸ A. D. Beyer, C. T. Chen, and N.-C. Yeh, submitted to Physica C; cond-mat/0610855.
 - ¹⁹ C.-T. Chen and N.-C. Yeh, Phys. Rev. B **68**, 220505 (2003).
 - ²⁰ H. Y. Chen and C. S. Ting, Phys. Rev. B **71**, 132505 (2005).
 - ²¹ B. Lake, G. Aeppli, K. N. Clausen, D. F. McMorrow, K. Lefmann, N. E. Hussey, N. Mangkorntong, M. Nohara, H. Takagi, T. E. Mason, et al., Science **291**, 1759 (2001).
 - ²² S. Chakravarty, H.-Y. Kee, and K. Volker, Nature **428**, 53 (2004).
 - ²³ H. Kotegawa, Y. Tokunaga, K. Ishida, G. q. Zheng, Y. Kitaoka, K. Asayama, H. Kito, A. Iyo, H. Ihara, K. Tanaka, et al., J. Phys. Chem. Solids **62**, 171 (2001).
 - ²⁴ H. Kotegawa, Y. Tokunaga, K. Ishida, G. q. Zheng, Y. Kitaoka, H. Kito, A. Iyo, K. Tokiwa, T. Watanabe, and H. Ihara, Phys. Rev. B **64**, 064515 (2001).
 - ²⁵ M. Naughton, J. Ulmet, A. Narjis, S. Askenazy, M. Charalala, and A. Hope, Rev. Sci. Inst. **68**, 4061 (1997).
 - ²⁶ D. S. Reed, N.-C. Yeh, M. Konczykowski, A. V. Samoilov,

- and F. Holtzberg, *Phys. Rev. B* **51**, 16448 (1995).
- ²⁷ M.-S. Kim, S.-I. Lee, S.-C. Yu, I. Kuzemskaya, E. Itskevich, and K. A. Lokshin, *Phys. Rev. B* **57**, 6121 (1998).
- ²⁸ A. Iyo, Y. Tanakaa, Y. Kodamaa, H. Kitoa, K. Tokiwab, and T. Watanabe, *Physica C* **445**, 17 (2006).
- ²⁹ J. L. O'Brien, H. Nakagawa, A. S. Dzurak, R. G. Clark, B. E. Kane, N. E. Lumpkin, N. Miura, E. E. Mitchell, J. D. Goettee, J. S. Brooks, et al., *Phys. Rev. B* **61**, 1584 (2000).
- ³⁰ N.-C. Yeh, W. Jiang, D. S. Reed, A. Gupta, F. Holtzberg, and A. Kussmaul, *Phys. Rev. B* **45**, 5710 (1992).
- ³¹ L. Krusin-Elbaum, T. Shibauchi, and C. H. Mielke, *Phys. Rev. Lett.* **92**, 097004 (2004).
- ³² The γ value for Hg-1245 was extrapolated from those of Hg-1201, Hg-1212, Hg-1223 and Hg-1234³³, with the latter three being comparable within experimental errors.
- ³³ D. Zech, J. Hofer, H. Keller, C. Rossel, P. Bauer, and J. Karpinski, *Phys. Rev. B* **53**, 6026 (1996).
- ³⁴ M.-S. Kim, C. U. Jung, S. I. Lee, and A. Iyo, *Phys. Rev. B* **63**, 134513 (2001).
- ³⁵ K. Tokiwa, H. Okumoto, T. Imamura, S. Mikusu, K. Yuasa, W. Higemoto, K. Nishiyama, A. Iyo, Y. Tanaka, and T. Watanabe, *Int. J. Mod. Phys. B* **17**, 3540 (2003).